ARCHIVIO ISTITUZIONALE
DELLA RICERCA

Alma Mater Studiorum Università di Bologna
Archivio istituzionale della ricerca

Preliminary Investigation of a Combined Heat and Power Reversible-Brayton System Integrated With a Renewable Power Source

This is the final peer-reviewed author's accepted manuscript (postprint) of the following publication:

Published Version:
Ancona M.A., Bianchi M., Branchini L., De Pascale A., Melino F., Ottaviano S., et al. (2023). Preliminary Investigation of a Combined Heat and Power Reversible-Brayton System Integrated With a Renewable Power Source. New York : American Society of Mechanical Engineers (ASME) [10.1115/GT2023-103125].

Availability:
This version is available at: https://hdl.handle.net/11585/954272 since: 2024-08-28

Published:
DOI: http://doi.org/10.1115/GT2023-103125

Terms of use:

Some rights reserved. The terms and conditions for the reuse of this version of the manuscript are specified in the publishing policy. For all terms of use and more information see the publisher's website.

This item was downloaded from IRIS Università di Bologna (https://cris.unibo.it/).
When citing, please refer to the published version.

(Article begins on next page)

15 September 2026

American Society of Mechanical Engineers

ASME Accepted Manuscript Repository

Institutional Repository Cover Sheet

First Last

ASME Paper Title: PRELIMINARY INVESTIGATION OF A COMBINED HEAT AND POWER REVERSI BRAYTON SYSTEM INTEGRATED WITH A RENEWABLE POWER SOURCE

Authors: Ancona M.A.; Bianchi M.; Branchini L.; De Pascale A.; Melino F.; Ottaviano S.; Peretto A.; Poletto C.

ASME Journal Title: Proceedings of ASME Turbo Expo 2023

Volume/Issue GT2023-103125, V008T16A005; 14 pages Date of Publication (VOR* Online) September 28, 2023

ASME Digital Collection URL: https://asmedigitalcollection.asme.org/GT/proceedings/GT2023/87028/V008T16A005/1168172

DOI: https://doi.org/10.1115/GT2023-103125

*VOR (version of record)

PRELIMINARY INVESTIGATION OF A COMBINED HEAT AND POWER REVERSIBLE-BRAYTON SYSTEM INTEGRATED WITH A RENEWABLE POWER SOURCE

Maria Alessandra Ancona
University of Bologna
Bologna, IT

Michele Bianchi
University of Bologna
Bologna, IT

Lisa Branchini
University of Bologna
Bologna, IT

Andrea De Pascale
University of Bologna
Bologna, IT

Francesco Melino
University of Bologna
Bologna, IT

Saverio Ottaviano
University of Bologna
Bologna, IT

Antonio Peretto
University of Bologna
Bologna, IT

Chiara Poletto
University of Bologna
Bologna, IT

ABSTRACT

Pumped Thermal Electricity Storage (PTES) technology is drawing increasing attention as a promising solution to limit the mismatch between the electric demand and the renewable production.

In this context, a preliminary model of a reversible Brayton PTES is developed on a commercial software to finalize a comprehensive performance investigation. In the proposed arrangement, the system allows to store the surplus of electric renewable production, by converting it into heat, through an inverse cycle, and then to convert it back into electric energy when needed, through a direct cycle. A systematic analysis comparing two configurations (base and recuperated) of the reversible Brayton system is carried out to assess the performance of the system.

Since thermal and electric energy flows are involved, PTES is particularly interesting when adopted to satisfy both thermal and electric demands, in a combined heat and power (CHP) system. To this aim, the system has been simulated when delivering both thermal and electric energy, in different partitioning. Results show that if 25 % of the stored heat is addressed to a thermal user the integrated system can be convenient in terms of saved primary energy, compared to conventional separate production. In case 70 % of the stored heat is delivered to a thermal user and 30 % reconverted into electricity, the maximum investment cost to have a return of the investment in 10 years is assessed to be between 2000 and 5000 €/kW, depending on the configuration.

.

Keywords: PTES, CHP, Brayton, Carnot batteries

NOMENCLATURE

Symbols

CF	cash flow
Ci	investment cost
E	energy
I	index
Q	heat

T	temperature
W	work

Subscripts

aux	auxiliaries
C	cold
ch	charge
comp	compressor
dis	discharge
el	electric
eq	equivalent
es	energy saving
H	hot
id	ideal
net	net
P	primary
P2P	power-to-power
r	discounted rate
ratio	ratio
ref	reference
ren	renewable
rt	roundtrip
t	time for the return of the investment
turb	turbine
th	thermal

Greek symbols

$\Delta\tau$	time period
η	efficiency

Abbreviations

BD	Brayton direct
BI	Brayton inverse
B-PTES	Brayton PTES
CAES	Compressed Air Energy Storage
CHP	Combined Heat and Power
COP	Coefficient Of Performance
EES	Electric Energy Storage
HTF	Heat Transfer Fluid
LAES	Liquified Air Energy Storage
NPV	Net Present Value
PHES	Pumped Hydro Energy Storage
PTES	Pumped Thermal Energy Storage
PR	Pressure ratio
RES	Renewable Energy Source
TES	Thermal Energy Storage
RECB-PTES	Recuperated Brayton PTES

1 INTRODUCTION

In order to reach carbon neutrality in less than 30 years, it is necessary to design a profound energy systems transformation in all the major carbon emitters sectors, namely industrial, residential and transportation. This transformation is based on a deep penetration of renewable energy sources (RES), which should almost totally replace the fossil fuel-based energy supply to reach the net-zero scenarios by 2050 [1]. However, the intrinsic instability and fluctuations of RES require not yet ready solutions to limit the mismatch between the RES production and the energy demand: the energy storage is among the major ones.

Although numerous solutions have been proposed for electricity storage, most of them are available for smaller scale rather than grid-scale electricity storage: among them, there are supercapacitors [2], flywheels [3], and batteries [4], which, due to their high cost per unit capacity, are not oriented towards long duration (from 4 to 8 h), as a grid-scale solution should be. Until today, the only grid-scale Electric Energy Storage (EES) technology that has proven to be technically and economically feasible is the Pumped Hydro Energy Storage (PHES) [5], whose easily-exploitable additional capacity is nearly exhausted [6]. Other EES technologies, which are drawing attention because of the use of inexpensive storage mediums, are the Compressed Air Energy Storage (CAES) and the so-called Carnot Batteries, which include technologies like the Pumped Thermal Energy Storage (PTES), the Liquified Air Energy Storage (LAES) and other concepts, like Lamm-Honigmann. CAES technology stores energy as compressed air in underground caverns [7], and can be upgraded increasing the efficiency up to 70 %, by adding a thermal storage: these systems are called adiabatic-CAES [1].

In contrast to PHES and CAES systems, Carnot Batteries are promising grid-scale solutions, not only because of their low specific cost and high energy density, but also due to the absence of geographical constraints, because they do not need pre-existing reservoirs and caves and they can be installed almost everywhere. Carnot Batteries working principle is based on the electric energy storage in form of heat: the renewable electricity production is converted into thermal energy in charging phase, to be recovered later during the discharging phase. In LAES technology, the electric input is used to liquefy air by compressing, cooling, and then expanding until liquefaction occurs: liquid air is then stored at atmospheric pressure [8].

In PTES, the charging phase occurs when an electric surplus is available: the electric energy is used as input to let heat flow against a thermal gradient, from a low temperature heat sink to a high temperature heat reservoir, thus, storing the electric surplus in form of thermal energy. The discharging phase typically occurs when electricity is required: the heat stored in the high temperature reservoir flows to the low temperature sink, powering a heat engine, for mechanical work production, which can be then converted into electric energy. As both thermal and electric energy flows are involved, PTES solutions seem to be promising when integrated in waste heat recovery (WHR) and combined heat and power (CHP) systems: the increase of very low-grade waste heat enthalpy content allows both to get better conversion efficiencies, in the discharging phase [9], and to supply to a thermal user heat at higher temperatures. Indeed, the thermal energy available in the storage may be not entirely reconverted into electricity, but used in some part to satisfy a thermal demand, introducing more flexibility even in the thermal production/consumption [10].

The technologies adopted to operate the charging/discharging phases may be several, depending on the temperature levels and on the application, but the most promising are based on direct and inverse Rankine cycle, and direct and inverse Brayton cycle.

In Rankine PTES, the charging phase is performed by a vapour compression heat pump, while the discharging phase is operated through a direct Rankine cycle, in which the stored heat is reconverted into mechanical power through a turbine or a volumetric expander [11]. Concerning the working fluid, different solutions can be found in literature, including water vapour [12], organic fluids [13], transcritical CO_2 [14 - 16], subcritical NH_3 [17]. In [18] a cascade system, using ammonia in a low temperature stage, and water in the high temperature stage, is investigated. Some studies have analyzed a system able to perform both the charging and the discharging phases with the same components, namely a reversible heat pump/Rankine cycle system, with a considerable reduction of the investment costs [5].

In Brayton PTES, a gaseous working fluid operates alternatively a (inverse) Brayton heat pump and a (direct) Brayton heat engine. During the charging phase (inverse cycle), the working fluid is compressed to high pressure and temperature, and then it releases the heat to a high temperature heat reservoir. During the discharging phase, the heat stored in charging mode is reconverted to mechanical work through an expansion process. In contrast to Rankine PTES, the system efficiency is more influenced by the temperature ratio and the machines polytropic efficiencies, rather than the pressure ratio [19]. Concerning the working fluids, the monoatomic gases argon and helium seem to be the most favourable choices: according to [20], helium should be preferred to argon as it results in a higher roundtrip efficiency (56.9 % against 39.3 % with argon). Furthermore, McTigue et al. [21] highlight that supercritical CO_2 cycles have higher work ratios and power densities than the systems based on ideal gases. Eventually, air allows to reach higher power output and efficiency, if an electric heater is included in the process [22]. Moreover, for Brayton PTES the possibility of employing the same devices [23], to perform both charging and discharging phases, has been investigated.

In this context, the purpose of this study is to investigate the thermodynamic performance of a closed Brayton PTES system in two promising configurations operating with supercritical CO_2, selected as a reference high-performing fluid according to previous literature. A parametric numerical analysis has been performed with a commercial software [24], in order to explore the potentiality of the proposed energy conversion and storage system: the analysed system

is investigated not only as an EES technology, but also as a solution to include more flexibility in the thermal production-demand match [25]. The discussion of the results has been carried out presenting, firstly the thermodynamic performance of the system in the charging and discharging phases, and as a whole, secondly the cogeneration characteristics when the PTES is adopted to satisfy both thermal and electric demands, in a CHP arrangement. Eventually, an economic analysis has been performed to evaluate the maximum specific investment cost that allows to have a return of the investment in a reasonable time period.
Some recent works have already investigated Brayton PTES systems, even considering different layouts [26, 27], but, to the Authors knowledge, a systematic analysis on the feasibility and the performance of a CHP Brayton PTES system, to limit the mismatch of both electric and thermal production-demand, still lacks in literature. In this context, Trevisan et al. [28] performed a techno-economic assessment of a recuperated s-CO2 Brayton Carnot battery considering four scenarios in terms of electricity market, and two specific industrial applications

1. MATERIALS AND METHODS

In this study, a reversible closed-cycle s-CO_2 Brayton PTES (B-PTES) is investigated to analyse its performance when integrated with a renewable energy source (RES). The system is supposed to work in a CHP scenario generating both thermal and electric energy according to the need. The conceived energy system concept is depicted in Figure 1, where the electric surplus of a renewable production is converted into heat through an inverse Brayton cycle; then the stored thermal energy can be sent to a thermal user, and/or reconverted into electricity when the demand exceeds the RES production. As schematized in figure 1, the B-PTES is composed of a thermal energy storage (TES), a Brayton inverse (BI) cycle system, and a Brayton direct (BD) cycle.

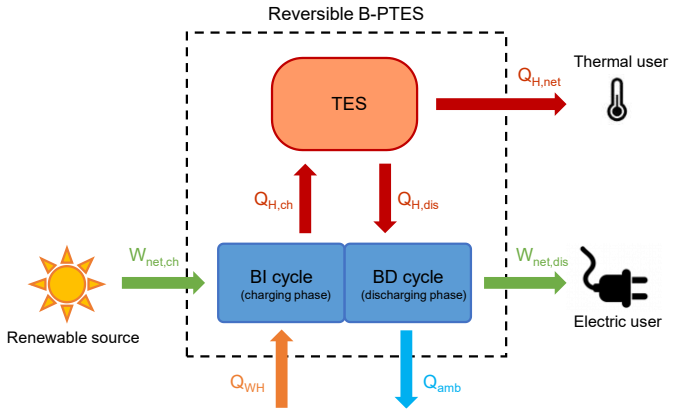

FIGURE 1: CONCEPTUAL SCHEME OF THE ENERGY SYSTEM UNDER INVESTIGATION

More in details, when the RES production exceeds the electric demand, the surplus ($W_{net,ch}$) is used to run the system in inverse mode, to store heat ($Q_{H,ch}$) in a hot reservoir; when the electric demand overcomes the RES production, the system operating mode switches to BD cycle, discharging heat ($Q_{H,dis}$) from TES to produce an extra electric output ($W_{net,dis}$). It can be beneficial to operate the BI cycle with a lower difference between temperature levels than the BD cycle, to increase the performance of the indirect cycle without affecting the direct cycle efficiency. This option can be realized if a cold source for the BI cycle is available at higher temperature than the cold sink of the BD cycle, i.e. if a free waste heat (Q_{WH}), not otherwise usable, is available. When the overall system production is lower than the demand, the deficit is covered by the grid. Furthermore, the availability of heat at relatively high temperature in the TES allows to partially cover a thermal user demand ($Q_{H,net}$), resulting in a CHP system, as it can store energy to satisfy both electric and thermal demands.

Therefore, on the electric side, the system can work in charging/discharging mode (BI and BD), while on the thermal side, the thermal discharge mode can be on or off regardless of the electric mode: even when the Brayton cycle is off, the Carnot Battery can work in pure thermal discharge.

2.1 Brayton PTES Configurations

Two layout configurations of the Brayton-PTES are considered in this study, namely a simple Brayton case (B-PTES) and a recuperated cycle case (RECB-PTES). Figure 2 illustrates components and flow streams of the B-PTES. In the charging phase (Figure 2(a)), the working fluid is firstly preheated at low pressure by a cold source in the cold

heat exchanger (Cold HX): the possibility of using available free low-temperature waste heat, which would not have been used otherwise (e.g., in many industrial processes residual heat is wasted with low enthalpy content) is preferable, according to [9]: it reduces the BI cycle temperature lift, increasing the system performance (the required compression work is reduced). Then the working fluid is compressed (in Compressor) and subsequently it releases high-temperature heat to TES (via Hot HX). In the last step of the closed BI cycle, the fluid is expanded back to the low pressure level (in Turbine), recovering part of the Compressor work. In the discharging phase (figure 2(b)) the cycle is reversed: the working fluid is compressed in Compressor; then it is heated by the hot source in the Hot HX; eventually it expands in Turbine, producing mechanical power, and it is cooled in the Cold HX, as last phase of the closed BD cycle.

A Recuperator (Rec HX) is added in the RECB-PTES configuration, as shown in Figure 3: in the BI cycle (Figure 3(a)), the Recuperator allows to reach higher temperature values at the Compressor inlet (point RC3), further post-heating the working fluid at the Cold HX outlet (RC2), with the fluid at the Hot HX outlet (RC5). In the BD cycle (Figure 3(b)), the Recuperator allows to pre-heat the working fluid at the inlet of the Hot HX (RD3) through the residual enthalpy content of the fluid at the Turbine outlet (RD5), with a benefit on the BD cycle conversion efficiency. In both layouts, TES consists in two reservoirs (Warm and Hot res.), in which a heat transfer fluid (HTF) performs the heat exchange and storage operations. Figure 4 and Figure 5 show the qualitative T-s diagrams of the BI and BD cycles in both the B-PTES and RECB-PTES cases. The operating fluid state points in the key points of the cycles are indicated with the Hot and Cold source temperature variations, for sake of comparison. To avoid loss of generality, no numerical values of temperatures, pressures, neither of other thermodynamic properties are provided.

As a result of a compromise between performance, availability and costs, supercritical CO_2 is chosen as working fluid for the current analysis. Furthermore, since its critical temperature is about 31 °C, it is possible to use low-grade cold sources and sinks, respectively in the BI and BD cycles. On the other hand, the fluid critical pressure (73.8 bar) requires relatively high-pressure levels, to keep the cycle in the supercritical regime, thus affecting the cycle pressure ratio in order to keep the cycle max pressure below the current technical limitations. This constraint affects the cycle maximum temperature, especially in the base configuration (Figure 4); the use of recuperator allows to increase the distance between the expansion and the compression processes (Figure 5), increasing the cycle maximum temperature and the TES temperature levels.

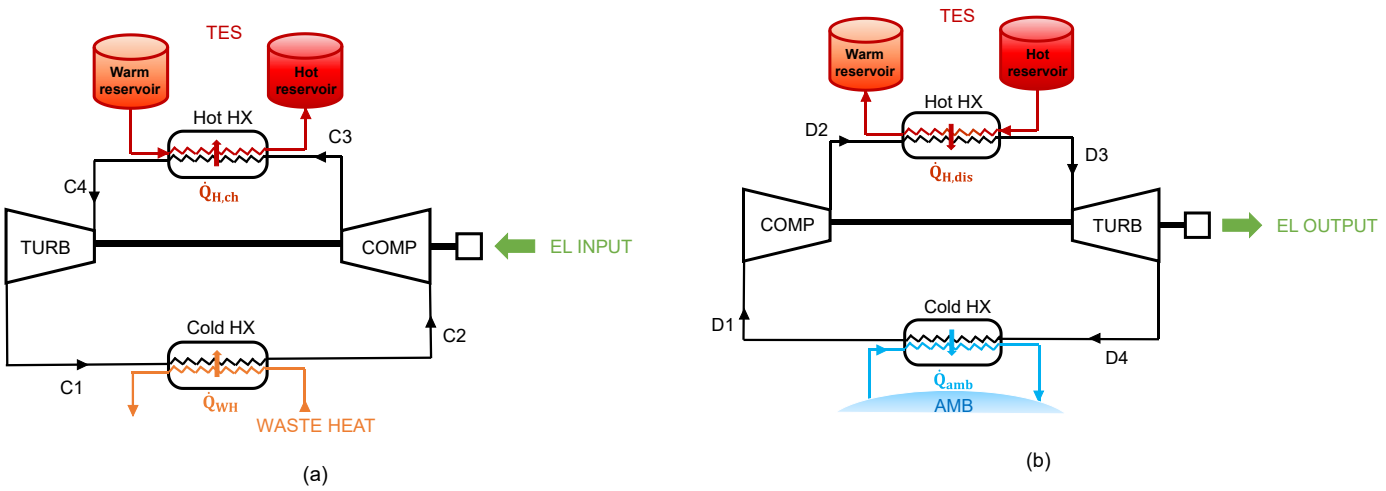

FIGURE 2: B-PTES LAYOUT IN (a) CHARGING AND (b) DISCHARGING MODE

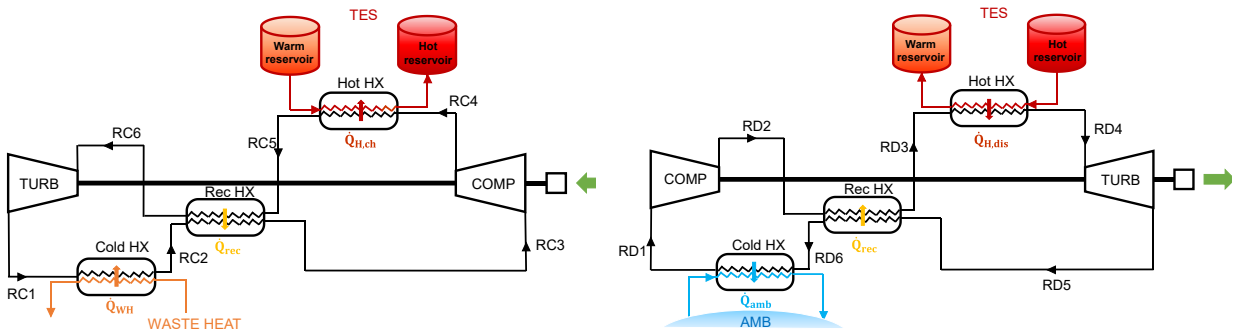

FIGURE 3: RECB-PTES LAYOUT IN (a) CHARGING AND (b) DISCHARGING MODE

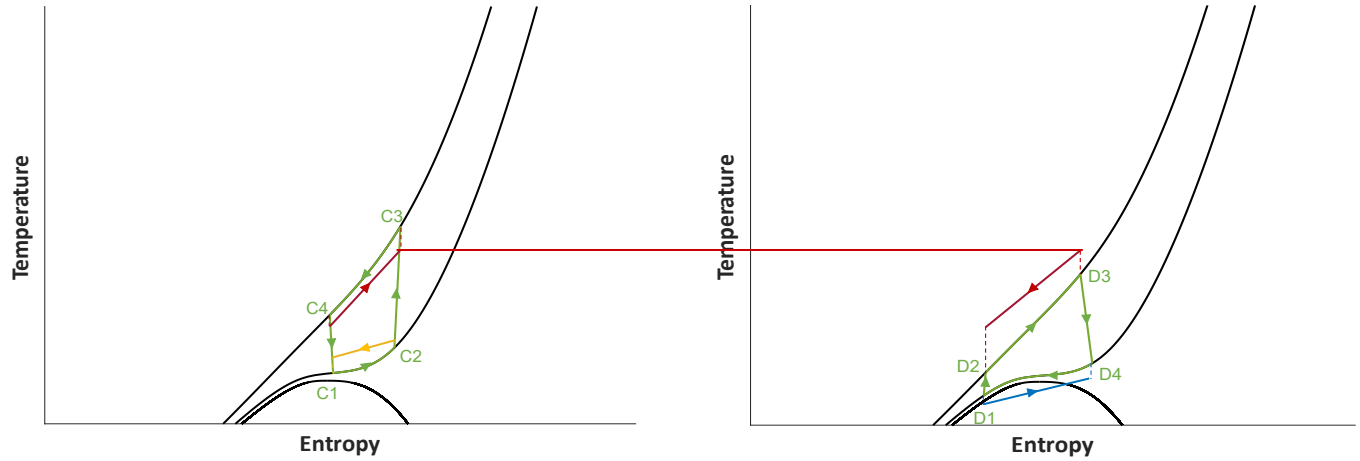

FIGURE 4: B-PTES QUALITATIVE T-s DIAGRAM IN (a) CHARGING AND (b) DISCHARGING MODE

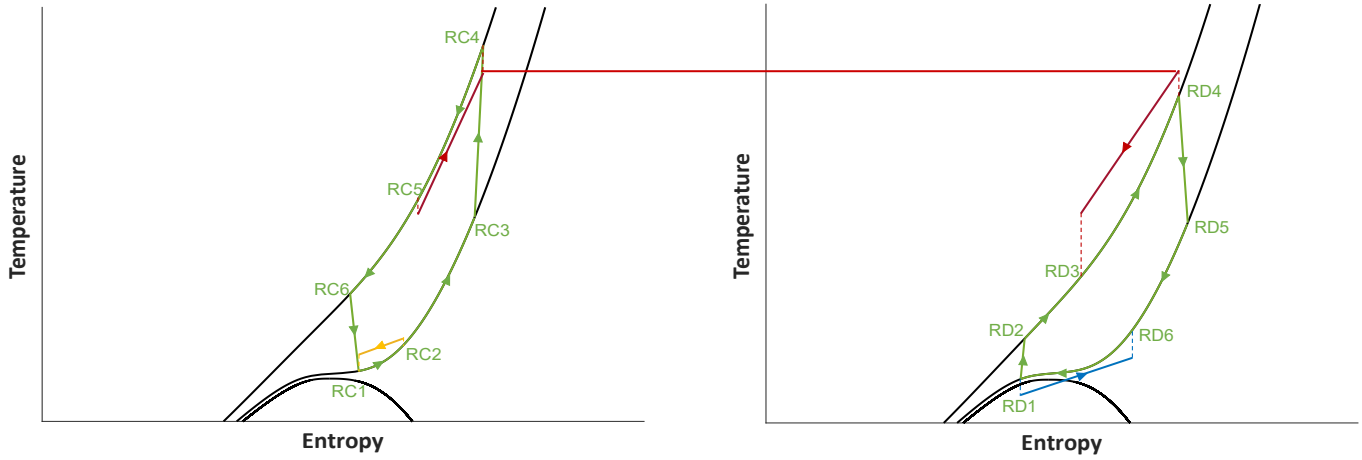

FIGURE 5: RECB-PTES QUALITATIVE T-s DIAGRAM IN (a) CHARGING AND (b) DISCHARGING MODE

2.2 Sensitivity analysis: modelling hypothesis and boundary conditions

The analysed power plant has been modelled by means of the commercial software THERMOFLEX [24], which allows for the thermodynamic modelling of complex energy systems, starting from built-in library single components assembly, through a lumped parameters approach. With this tool, CO_2 and secondary fluids properties are evaluated according to Refprop thermodynamic database [29].

A sensitivity thermodynamic analysis has been carried out to investigate the performance variation of the B-PTES and RECB-PTES system configurations, under different design settings, mainly in terms of the heat sources temperature levels and the turbomachines pressure ratio (PR) values.

Concerning the hot source temperature level, the Hot HX HTF inlet temperature (coming from the TES warm reservoir) has been set as input, and the outlet temperature has been calculated. In particular, in the base configuration, three levels of the HTF inlet temperature, namely 70 °C, 85 °C and 100 °C, have been considered. Assumed TES temperature values are in line with a medium/low-grade heat user demand and they are compatible with the maximum temperature obtained with the B-PTES at the outlet of the compressor in charging mode (within the investigated range of pressure values, the resulting C3 point temperature values are not higher than 200 °C). In the RECB-PTES case, the HTF inlet temperature has been varied, setting it equal to 150 °C, 250 °C and 350 °C; indeed, with the recuperator, it is possible to increase the cycle maximum temperature (point RC4) up to 550 °C. In this case, the considered TES temperature levels fit with typical industrial medium/high-grade heat users. The HTFs have been chosen taking into account their temperature limits and fitting with the cycle operating temperature levels:

TABLE 1: HYPOTHESIS AND BOUNDARY CONDITIONS

Hot and Cold sources boundary conditions	**B-PTES**		**RECB-PTES**	
	charging	**discharging**	**charging**	**discharging**
Hot sink/source fluid	Duraterm630		Helisol5A / Nitrate Salt 60% NaNO3 - 40% KNO3	
Inlet temperature	[70 – 85 – 100] °C	--	[150 – 250 – 350] °C	--
Outlet temperature	--	[70 – 85 – 100] °C	--	[150 – 250 – 350] °C
Cold source/sink fluid	Water			
Mass flow rate	1.5 kg/s			
Inlet temperature	60 °C	20 °C	60 °C	20 °C

- in the base configuration, in which temperatures are never higher than 200 °C, Duratherm 630 (maximum operating temperature of 329 °C) has been chosen as HTF;
- in the recuperated configuration, in the cases of the first two levels of temperatures (150 and 250 °C), Helisol 5A (maximum operating temperature of 450 °C) has been set as HTF;
- for the third level of temperature, nitrate salt (minimum operating temperature of 260 °C, maximum operating temperature of 593 °C) has been selected.

The cold source/sink has been simulated considering water as external fluid, and the water inlet temperature at the Cold HX equal to 60 °C and 20 °C, respectively in the charging and discharging phases. In particular, in the charging mode, it has been assumed that very low-grade heat is recovered from an external (waste) heat source and exploited as free energy source; in the discharging mode, water close to ambient conditions is considered as cold sink. The choice of diversifying the low-temperature level, at the BI and BD cycles, lie in the fact that the analysed storage system is justified only if applied to already existing technologies to reduce waste energy. The thermal integration allows both to recover waste heat, (e.g. in an industrial process) that would otherwise be discharged to the ambient, and to increase the charging phase performance, because it allows to reduce the temperature lift that the compressor has to win, resulting in a lower electric consumption.

All the hypothesis and boundary conditions about the hot and the cold sources are listed in Table 1.

Concerning the operating pressure levels of the reversible Brayton cycles, a parametric analysis has been carried out under the following hypothesis:

- the low-pressure level has been set to 80 bar (slightly above the CO_2 critical pressure), in order to obtain supercritical conditions of the fluid in all the cycle sections, in both the charging and discharging phases;
- the high-pressure level has been varied in order to identify the optimal PR value;

- nevertheless, the BI and BD cycles maximum pressure is bounded to 350 bar to comply with current technological limits. As a result, the cycle PR value has been systematically varied in the range from 1.5 to 4.25, with a step of 0.25;
- the PR value of the BI and the BD cycles are considered equal for the same system thermodynamic design, for sake of simplicity.

The turbine and compressor polytropic efficiency values are kept constant, and both set equals to 85 %, in line with data available in literature [21, 30]. The heat exchangers effectiveness, minimum pinch point, normalized heat loss and pressure drop values are set equal for all the heat exchangers in both the configurations, and reported in Table 2.

TABLE 2: SYSTEM MAIN SPECIFICS

B-PTES and RECB-PTES main specifics	
Operating fluid	Carbon Dioxide
Mass flow rate	1 kg/s
Compressor inlet pressure	80 bar
Maximum pressure limit	350 bar
Pressure ratio	from 1.5 to 4.25 with a step of 0.25
Compressor polytropic efficiency	85 %
Turbine polytropic efficiency	85 %
Mechanical efficiency	99 %
Auxiliary efficiency	99 %
Generator / Motor electric efficiency	90 %
Heat exchangers thermal effectiveness	90 %
Heat exchangers minimum pinch point	5 °C
Heat exchangers normalized heat loss	1 %
Pressure drops across heat exchangers	2 %

Concerning the economic analysis, the maximum investment cost is evaluated for a return of the investment in 10 years, considering a discounted rate of 0.06 [31]. The cash flows have been calculated assuming 1500 equivalent working hours of the RES [32], an yearly average electricity price of 0.30 €/kWh [33], and an yearly average thermal energy price of 0.18 €/kWh [34], both in line with the average prices in several European countries in 2022. The maximum investment cost has been estimated varying alternatively the electricity and the thermal energy prices: the former has been varied in the range between 0.05 and 0.40 €/kWh, the latter in the range between 0.03 and 0.24 €/kWh. The hypothesis adopted for the economic analysis are summarized in Table 3.

TABLE 3: ECONOMIC SPECIFICS

Specifics for the economic analysis	
Time for the return of the investment	10 years
Discounted rate	6 %
RES equivalent working hours	1200 h
Reference electricity price	to 0.30 €/kWh
Reference thermal energy price	to 0.18 €/kWh
Electricity price variation range	From 0.05 to 0.40 €/kWh with a step of 0.05
Thermal energy price variation range	From 0.03 to 0.24 €/kWh with a step of 0.03

2.3 Performance Indexes

In order to perform a systematic analysis evaluating the operation of the Brayton PTES system, and comparing the two configurations, some relevant performance indexes are introduced in this study, related to the charging mode, the discharging mode and the overall operation, as specified below.

The considered indexes related to the performance of the charging phase are as follows:

- The inverse cycle output heat per unit of working fluid mass flow rate ($Q_{H,ch}$), stored in the hot reservoir; this index represents the output thermal production of the system during the charging mode.
- The input net specific electric work ($W_{net,ch}$) of the inverse cycle, calculated as:

$$W_{net,ch} = \frac{(W_{comp} - W_{turb})}{\eta_{aux}} \quad (1)$$

where W_{turb} is the turbine specific work, W_{comp} the compressor specific work, and η_{aux} the plant auxiliary efficiency, which includes the losses due to electric and mechanic auxiliaries. This quantity measures the amount of renewable electric energy in surplus stored in the Carnot battery.

- The coefficient of performance (COP) evaluates the thermodynamic performance of the inverse cycle and it is calculated as:

$$COP = \frac{Q_{H,ch}}{W_{net,ch}} \quad (2)$$

where $W_{net,ch}$ is the net specific electric consumption and $Q_{H,ch}$ is the output thermal production of the system during the charging mode. In presence of free waste heat, available at a temperature value higher than ambient temperature, the compressor operates with a lower temperature lift, $W_{net,ch}$ decreases, and COP increases in presence of free waste heat.

The calculated COP values can be compared with the ideal coefficient of performance (COP_{id}), defined as follows:

$$COP_{id} = \frac{T_{H,eq}}{T_{H,eq} - T_{C,eq}} \quad (3)$$

where $T_{H,eq}$ and $T_{C,eq}$ are the average temperature values of the working fluid during the heat release and absorption phases [35].

The considered indexes related to the performance of the discharging phase are as follows:

- The delivered heat ($Q_{H,dis}$) from the hot reservoir into the direct cycle, per unit of working fluid mass flow rate. This quantity represents the thermal energy stored in the charging phase, that is reconverted into electric energy.
- The output net specific electric work ($W_{net,dis}$) of the direct cycle, calculated as:

$$W_{net,dis} = (W_{turb} - W_{comp}) \cdot \eta_{aux} \quad (4)$$

This quantity represents the system electric output, sent to an electric user, during the discharging phase.

- The net electric efficiency of the direct cycle (η_{dis}), calculated as:

$$\eta_{dis} = \frac{W_{net,dis}}{Q_{H,dis}} \quad (5)$$

η_{dis} can be compared with the Carnot efficiency (η_{Carnot}):

$$\eta_{Carnot} = 1 - \frac{T_{C,eq}}{T_{H,eq}} \quad (6)$$

The indexes used to discuss the performance of the integrated system, namely of the whole storage and return process, are:

- The roundtrip efficiency (η_{rt}), calculated as a function of COP, η_{dis} and of the TES efficiency (η_{TES}), which includes the thermal energy storage dissipations, according to:

$$\eta_{rt} = COP \cdot \eta_{dis} \cdot \eta_{TES} \quad (7)$$

In this study, for the sake of simplicity, a constant value of η_{TES} equal to 99 % has been assumed. The ideal value of the roundtrip efficiency ($\eta_{rt,id}$), as a comparison term, is computed as follows:

$$\eta_{rt,id} = COP_{id} \cdot \eta_{Carnot} \quad (8)$$

- The time ratio ($\Delta\tau_{ratio}$) is the ratio between the time needed to completely discharge the storage ($\Delta\tau_{dis}$) and the time needed to charge it ($\Delta\tau_{ch}$):

$$\Delta\tau_{ratio} = \frac{\Delta\tau_{dis}}{\Delta\tau_{ch}} = \frac{Q_{H,ch}}{Q_{H,dis}} \quad (9)$$

This quantity is calculated as the ratio between $Q_{H,ch}$ and $Q_{H,dis}$, assuming that the overall amount of thermal energy stored in charging phase must be equal to the overall amount of thermal energy released in discharging phase.

Finally, the system performance is also analysed considering that the stored heat can be both used to satisfy a thermal demand or reconverted into electricity. In order to evaluate the system CHP performance, the following quantities are also considered:

- The net heat output ($Q_{H,net}$), representing the energy provided to the thermal user from the hot reservoir, evaluated as:

$$Q_{H,net} = Q_{H,ch} - Q_{H,dis} = Q_{H,ch} - \frac{W_{net,dis}}{\eta_{dis}} \quad (10)$$

- The primary energy reference consumption associated to the net heat output ($E_{P,th}$) and the primary energy reference consumption associated to the net electric output ($E_{P,el}$), calculated respectively as:

$$E_{P,th} = \frac{Q_{H,net}}{\eta_{th,ref}} \quad (11)$$

$$E_{P,el} = \frac{W_{net,dis}}{\eta_{el,ref}} \quad (12)$$

where the reference thermal efficiency ($\eta_{th,ref}$), and the reference electric efficiency ($\eta_{el,ref}$) are considered equal to 90 % and 52.5 % respectively, according to the EU legislation [36] for CHP plants.

- In particular, to compare the system energy production with conventional generation of heat and power, a simplified energy saving index (I_{es}) is introduced in this study, calculated as:

$$I_{es} = \frac{E_{P,th} + E_{P,el} - W_{ren}}{W_{ren}} \quad (13)$$

where W_{ren} is the primary energy input to the system (for the sake of simplicity $W_{ren} = W_{net,ch}$, as the input power is considered renewable). This index represents the normalized primary energy saved by producing heat and power with the system in study, instead of using conventional energy systems. When the index is greater than zero, the integrated system is expected to provide a gain in terms of primary energy consumption, with reference to conventional separate systems for heat and electricity production.

In this study the I_{es} is evaluated for different combinations of final allocation of the TES available energy, between the electricity demand and the thermal demand: in other words, the heat available in the reservoirs can be i) completely sent to the thermal user, or ii) completely converted into electricity to cover the electric demand, or iii) partially sent to the thermal user and partially converted into electricity (in several partitioning solutions).

Eventually, the maximum specific investment cost (Ci) of the system to guarantee a return of the investment in 10 years is evaluated through the Net Present Value (NPV):

$$NPV = \sum_{j=1}^{t} \frac{CF_j}{(1+r)^j} - Ci \quad (14)$$

where CF_j is the cash flow of the j-th year, r is the discount rate factor, and t is equal to 10 years.

2. RESULTS AND DISCUSSION

This paragraph presents and discusses the results of the comparative analysis between the B-PTES and the RECB-PTES system.

The first presented results are related i) to the thermodynamic performance of the system in the charging and discharging phases, and ii) to the thermodynamic performance of the integrated system. A comparison with the ideal system is performed. The hot reservoir temperature achievable in each case is showed to provide an idea of the temperature level at which the thermal energy is provided to the user. Then, thermal and electrical production, respectively in charging and discharging phases, are compared for the two system configurations. After that, the cogeneration characteristics of the integrated system are evaluated and discussed. Eventually, the maximum investment cost of the system, to obtain a return of the investment within 10 years, is estimated when varying alternatively the electricity and the thermal energy prices: the results are discussed and compared.

3.1 Thermodynamic performance

In Figure 6, COP of the BI, η_{dis} of the BD and η_{rt} are compared for the B-PTES (a) and RECB-PTES (b) configurations.

The COP values are higher in the base configuration because the temperature lift between the cold source and the hot sink is much lower compared to the recuperated configuration; however, the low hot temperature strongly affects the discharging efficiency, especially in the base configuration, in which the high temperature level is limited: indeed, η_{dis} reaches more acceptable values in the RECB-PTES. Furthermore, since the explored temperature levels in the B-PTES case are quite similar, η_{dis} curves are almost overlayed. The cycle PR value has a more significant effect on the COP of the base case, in which optimal values are assessed to be between 2.25 and 3.25 (depending on the temperature level), than the recuperated configuration, in which the charging phase performance are almost constant when varying the pressure ratio; the η_{dis} value increases with PR, as expected, for both the simple and the recuperated cycle.

Eventually, η_{rt} reaches higher values in the RECB-PTES configuration, where the maximum values, with the highest PR values, are assessed to be around 35 %, while the maximum roundtrip efficiency is less than 20 % without the recuperator. The roundtrip efficiency is strongly penalised by the discharging efficiency, rather than by the COP, especially in the B-PTES configuration: indeed, the resulting COP values are in line with high temperature heat pump (HTHP) literature values [37].

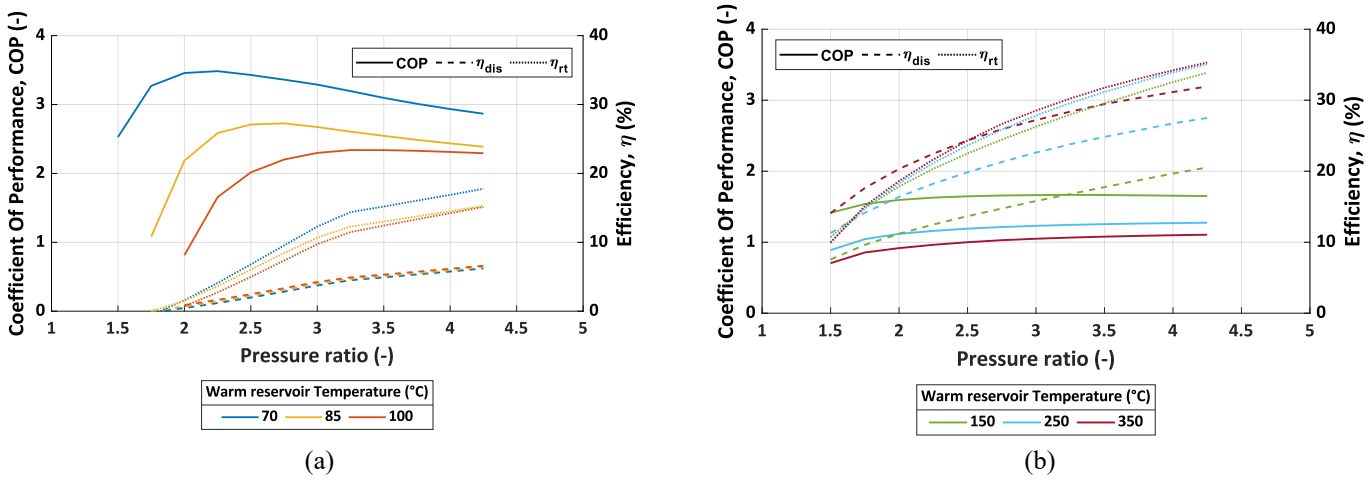

FIGURE 6: COEFFICIENT OF PERFORMANCE (COP), NET ELECTRIC EFFICIENCY (η_{dis}), ROUNDTRIP EFFICIENCY (η_{rt}) IN (a) BASE AND (b) RECUPERATED CONFIGURATIONS, VERSUS PRESSURE RATIO

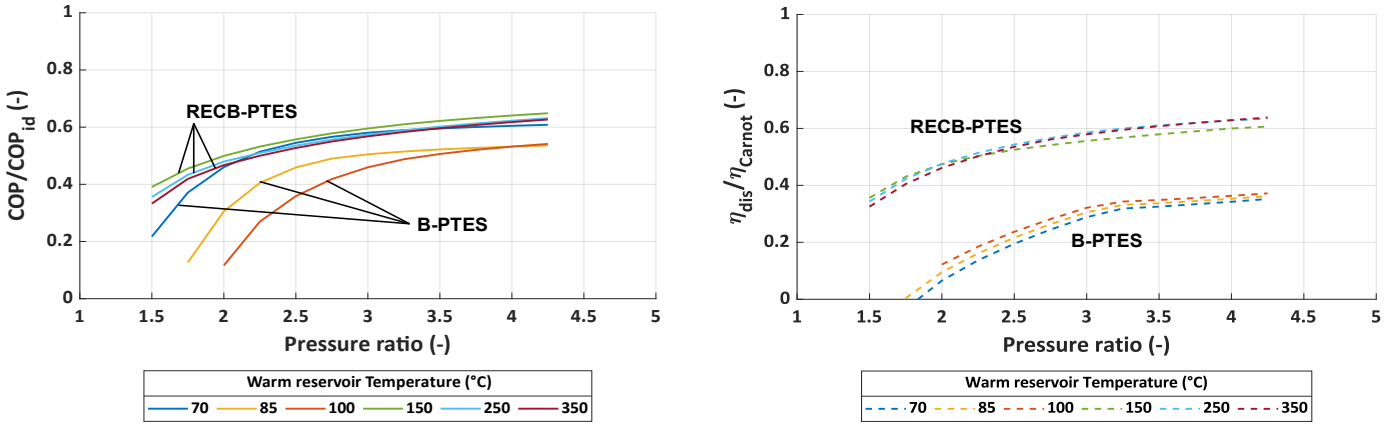

FIGURE 7: PERFORMANCE COMPARISON: RATIO BETWEEN THE COP AND THE IDEAL COP (a), AND RATIO BETWEEN THE DISCHARGING EFFICIENCY AND CARNOT EFFICIENCY (b), VERSUS PRESSURE RATIO

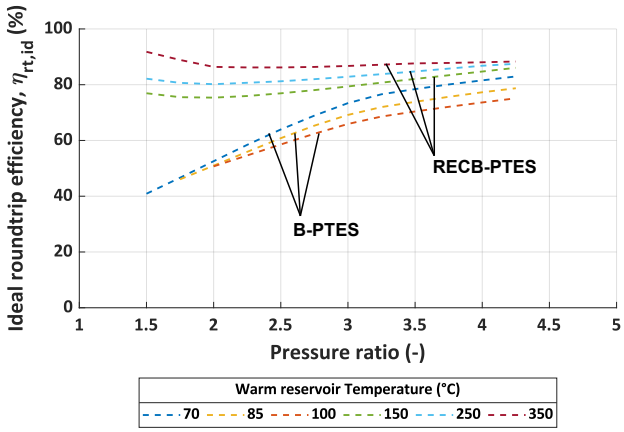

FIGURE 8: IDEAL ROUNDTRIP EFFICIENCY VERSUS PRESSURE RATIO

Furthermore, Figure 7(a) shows that the COP value is at least 50 % of the ideal COP for almost all the cases, except for those at very small PR, while the discharging efficiency (Figure 7(b)) is significantly lower than the Carnot efficiency in the base configuration, never reaching 40 % of η_{Carnot}. In addition, in the B-PTES configuration, even the ideal roundtrip efficiency (Figure 8) does not reach significantly high values, especially for the low PR values. In any case, $\eta_{rt,id}$ never reaches values higher than 100 %, although in some studies [38] the thermal integration allows to overcome this value: this is probably due to the very low temperature (< 60 °C) at which the waste heat is provided to the inverse cycle.

Figure 9 shows the TES hot reservoir temperature obtainable for the six considered temperature levels (three for the B-PTES and three for the RECB-PTES) versus PR. With the base configuration, the maximum achievable temperature of the heat stored in the hot reservoir is lower than 200 °C, and it seems that it depends almost only on PR, rather than on the heat sink temperature level (warm reservoir). On the contrary, in the recuperated configuration, the temperature of the heat achieved in charging phase is strongly affected by the HTF temperature in the warm reservoir, namely at the beginning of the heat transfer process. In the RECB-PTES the maximum achievable temperature is assessed to be more than 550 °C.

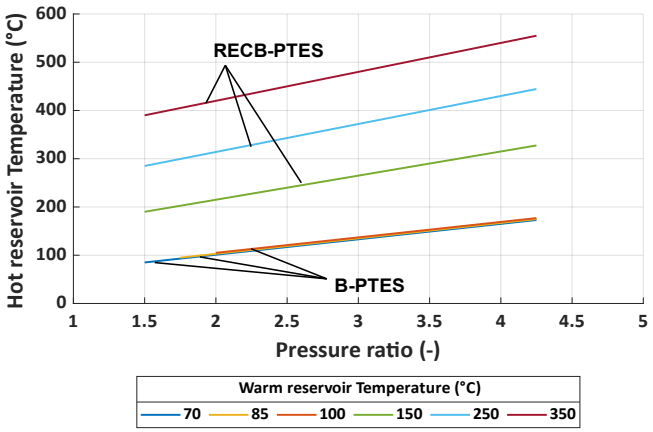

FIGURE 9: HOT RESERVOIR TEMPERATURE, OBTAINABLE FOR EACH ANALYZED LEVEL OF WARM RESERVOIR TEMPERATURE, IN BOTH THE CONFIGURATIONS, VERSUS PRESSURE RATIO

3.2 Thermal and electric production

The inverse cycle output heat ($Q_{H,ch}$) and the delivered heat from the hot reservoir into the direct cycle ($Q_{H,dis}$) are represented in Figure 10(a). Input net specific electric work ($W_{net,ch}$), during the charging phase, and output net specific electric work, during the discharging phase ($W_{net,dis}$), are represented in Figure 10(b). Results show that $Q_{H,ch}$ is always lower than $Q_{H,dis}$. To return, in the discharging phase, the same amount of thermal energy accumulated during charging phase, two approaches can be identified: i) a first solution is playing with the working fluid mass flow rate, by increasing it during charging mode and/or decreasing its value during discharging operations; ii) another solution is to consider different charging and discharging time. In other words, with the same working fluid mass flow rate value, the time needed to charge the TES is always higher than the time requested to completely discharge it. The first approach is trivial, as the produced/absorbed thermal power varies directly with the working fluid mass flow rate.

The second solution involves the calculation of the time ratio ($\Delta\tau_{ratio}$), namely the time needed to discharge the storage, with reference to the time necessary to charge it, which is represented in Figure 11. The $\Delta\tau_{ratio}$ value increases with PR and it overcomes 0.8 in the two cases at the lowest temperature level (Figure 12) for the two configurations (respectively 70 °C and 150 °C): indeed, these are the cases with the highest COP value, i.e. with the maximum $Q_{H,ch}$ for B-PTES and RECB-PTES, and with the lowest $Q_{H,dis}$ in the discharging phase. Therefore, Figures 11 and 12 show that the time ratio decreases with the warm reservoir temperature and increases with the pressure ratio. The variation of this parameter is more significant in the B-PTES configuration, rather than in the RECB-PTES, especially for the lowest values of the PR.

3.3 Preliminary cogeneration performance evaluation

Part of the heat stored in the TES, instead of being reconverted into electricity, may be directly sent to a thermal user, increasing the flexibility of the system while matching production and demand in specific application cases. More in details, depending on the user demand profiles, the stored energy in the TES can be differently partitioned between the thermal user and the electric user (via the reconversion through the BD cycle), resulting in different CHP scenarios.

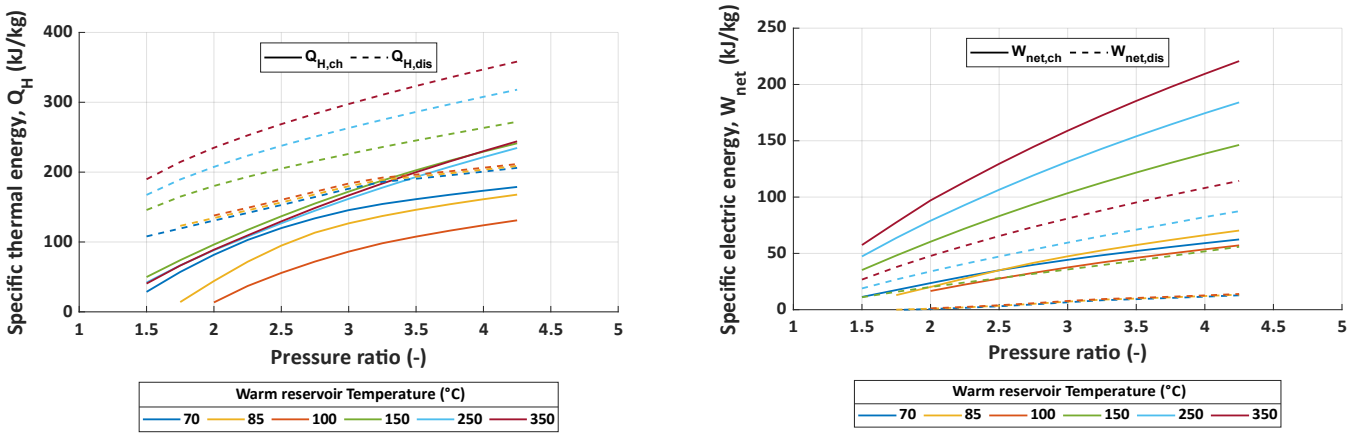

FIGURE 10: SPECIFIC THERMAL ENERGY (a) PRODUCED IN CHARGING MODE ($\dot{Q}_{H,ch}$) AND ABSORBED IN DISCHARGING MODE ($\dot{Q}_{H,dis}$), AND SPECIFIC ELECTRIC ENERGY (b) ABSORBED IN CHARGING MODE ($\dot{W}_{net,ch}$) AND PRODUCED IN DISCHARGING MODE ($\dot{W}_{net,dis}$), VERSUS PRESSURE RATIO

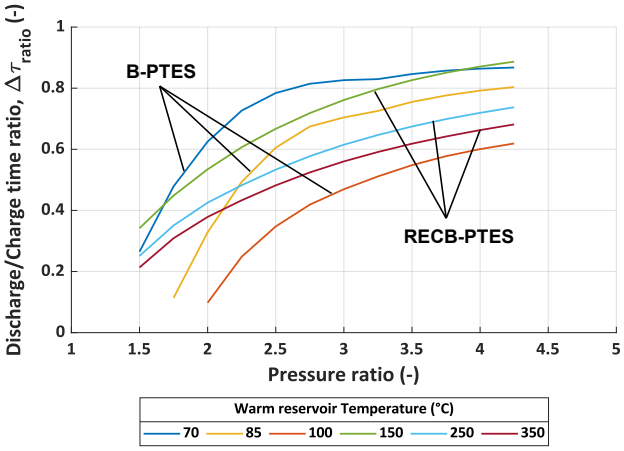

FIGURE 11: DISCHARGE/CHARGE TIME RATIO VERSUS PRESSURE RATIO, FOR THE SIX LEVELS OF WARM RESERVOIR TEMPERATURE

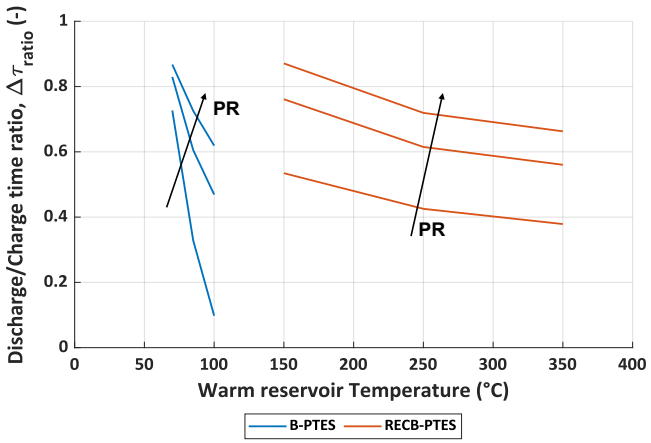

Figure 12: DISCHARE/CHARGE TIME RATIO VERSUS THE WARM RESERVOIR TEMPERATURE, FOR DIFFERENT VALUES OF THE PRESSURE RATIO, FOR THE TWO ANALYZED CONFIGURATIONS

In this study, for the sake of generality, a parametric analysis is performed in order to consider different possible scenarios in terms of the heat-to-power production ratio. The whole range of possible values is taken into account, by varying the available TES heat partitioning, from 100 % directly sent to the thermal user (0 % to the electric user), to 100 % reconverted into electricity to satisfy the electric demand. In each condition the specific energy saving index (I_{es}) is evaluated, in order to assess the convenience of adopting the proposed system integrated with a RES power plant (e.g., PV panels), in comparison with conventional heat and power separate production systems. Figure 13 shows the I_{es} calculated values for each temperature level of both configurations. In particular a PR value has been taken for each PTES configuration according to COP maximum value (see Figure 6).

Results, presented in Figure 13, show that, for higher percentage of heat reconverted into electricity, the analysed system is not convenient in terms of I_{es}, compared to the conventional separate production. Indeed at least 60 % of the TES available heat needs to be addressed to thermal user (maximum 40 % of heat reconverted into electricity) to guarantee a positive value of I_{es} in both configurations, for all the levels of temperature. More in details, the B-PTES configuration shows higher I_{es} values than the RECB-PTES: B-PTES provides a benefit up to 70 – 75 % of stored heat reconversion into electricity for all the three temperature levels, while RECB-PTES is slightly convenient compared to the separate production with maximum 65 % of thermal energy reconversion, in the case at the lowest temperature level (150 °C), and 50 % and 60 % respectively at 250 °C and 350 °C. Therefore, Figure 13 shows that the higher is the temperature level, the higher needs to be the percentage of available thermal energy addressed to a thermal user. Moreover, the cases with lower warm reservoir temperature values provide higher values of the primary energy saving index.

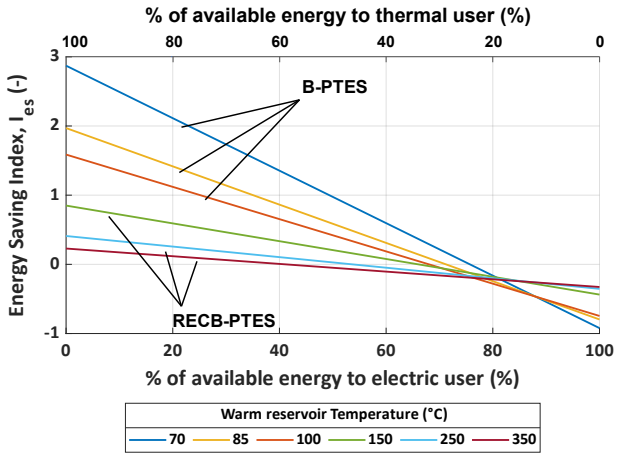

FIGURE 13: ENERGY SAVING INDEX EVALUATED IN THE WHOLE RANGE OF STORED ENERGY PARTITIONING BETWEEN THE ELECTRIC USER AND THE THERMAL USER, FOR THE SIX LEVELS OF TEMPERATURE

3.4 Economic analysis

The economic convenience of the system has been evaluated calculating the maximum specific investment cost that would guarantee a return of the investment in a reasonable time period, which has been set equal to 10 years. The analysis has been performed for both configurations (B-PTES and RECB-PTES) at all the temperature levels, selecting a PR value for each case. The maximum specific investment cost has been calculated in two scenarios: one in which 30 % of the TES available heat is reconverted into electricity, and the other in which 70 % of the TES heat is reconverted into electricity. The specific investment cost is evaluated varying alternatively the electricity price and the thermal energy price, resulting in a sensitivity analysis on energy price variation.

Figure 14 shows the maximum specific investment cost (Ci) for each case when varying the average electricity price. Figure 14(a) shows that when most of the available energy is addressed to the thermal user, the maximum specific investment cost is almost not affected by the electricity price variation: the highest Ci is obtained with the B-PTES configuration at the lowest temperature level, and it is assessed to be about 5000 €/kW. When most of the available energy (70 %) is reconverted into electricity (Figure 14(b)), the price variation slightly influences the specific investment cost, especially in the recuperated configuration: Ci varies between about 1000 and 2000 €/kW. Comparing the two graphs in Figure 14, it is possible to notice that the system is still convenient, and the specific investment cost can be higher, in case most of the produced thermal energy is directly used: this is in line with the linear trend of the energy saving index. The I_{es} trend is also coherent with the higher convenience of the B-PTES configuration instead of the RECB-PTES. Reasons lie in the stronger weight that the charging phase (and the COP) has in the improvement of the roundtrip efficiency in the B-PTES rather than in the RECB-PTES (Figure 6). In the recuperated configuration the discharging phase (and the discharging efficiency) gains importance in the improvement of the roundtrip efficiency, so the electricity price variation has a stronger influence on the return of the investment. In any case, an increase in the price makes convenient systems with a higher specific investment cost.

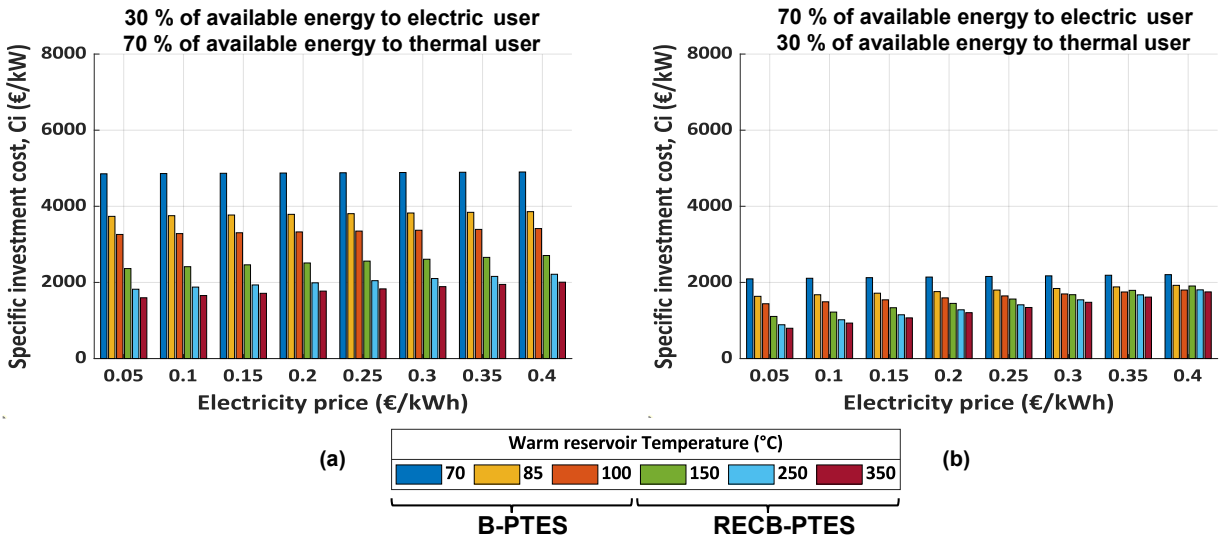

FIGURE 14: MAXIMUM INVESTMENT COST OF THE SYSTEM TO HAVE THE RETURN OF THE INVESTMENT WITHIN 10 YEARS WHEN VARYING THE AVERAGE ELECTRICITY PRICE OF (a) 30 % OF AVAILABLE THERMAL ENERGY RECONVERTED INTO ELECTRICITY AND (b) 70 % OF AVAILABLE THERMAL ENERGY RECONVERTED INTO ELECTRICITY

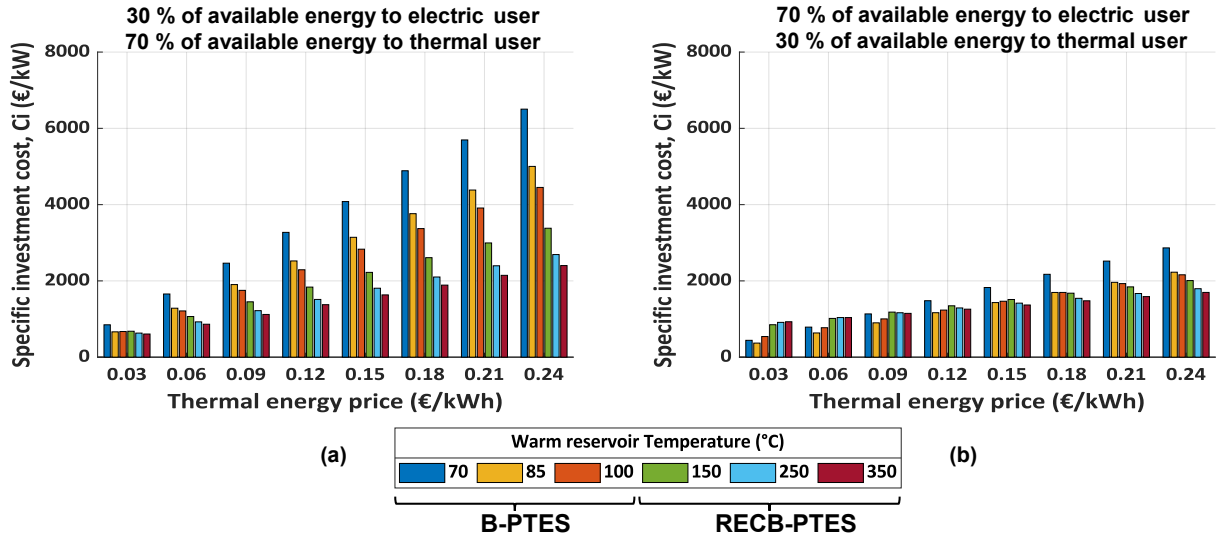

FIGURE 15: MAXIMUM INVESTMENT COST OF THE SYSTEM TO HAVE THE RETURN OF THE INVESTMENT WITHIN 10 YEARS WHEN VARYING THE AVERAGE THERMAL ENERGY PRICE OF (a) 30 % OF AVAILABLE THERMAL ENERGY RECONVERTED INTO ELECTRICITY AND (b) 70 % OF AVAILABLE THERMAL ENERGY RECONVERTED INTO ELECTRICITY

Figure 15 shows the maximum Ci when varying the average thermal energy price. The convenience of a system with such a specific investment cost is strongly dependent on the thermal energy price, especially for the B-PTES configuration, in which the thermal production has a major weight in the performance: in this case, at the lowest level of temperature Ci varies from less than 1000 to more than 6000 €/kW, depending on the thermal energy price. Furthermore, when most of the available thermal energy is reconverted into electricity (Figure 15(b)), and in case of low thermal energy price, the RECB-PTES configuration shows a higher maximum specific investment cost (more

than 1000 €/kW) than the B-PTES (less than 500 €/kW): this is due to the higher weight the discharging phase, and so the electricity production, has on the system.

3. CONCLUSIONS

In the effort to push towards the decarbonization of the energy sector and to increase the penetration of renewable energy sources, it is necessary to develop strategies to absorb their instability and fluctuations, allowing for more flexible use. PTES technology, based on the reversible Joule-Brayton cycle may be included among solutions.

This paper presents a systematic thermodynamic comparison between a closed Brayton-PTES in its base configuration, and a recuperated version, in which an additional heat exchanger (a recuperator) allows to obtain higher cycle maximum temperatures (even higher than 500 °C), increasing the distance between the expansion and the compression processes. Although the highest roundtrip efficiencies (20 – 30 %) are reached in the recuperated configuration, due to the higher discharging efficiencies, the COP of the inverse cycle is higher in the base configuration, because of the lower temperature lift: indeed, it reaches values of even 3.5, against less than 2 in the recuperated configuration. The cogeneration performance has been included in the analysis, considering that part of the heat available in the storage can be directly sent to a thermal user: results show that, in the best case (heat temperature level at 70 °C), at least 25 % of the stored heat should be addressed to a thermal user to make the integrated system convenient in terms of saved primary energy, compared to conventional separate production. The thermal production needs to be at least 60 % to obtain a positive specific energy saving index at the highest temperature level (350 °C). Eventually, the maximum specific investment cost of the system in the two analysed configurations, to have the return of the investment within 10 years, has been evaluated when varying alternatively the average electricity and thermal energy prices: results show an increase in the allowed maximum specific investment cost when increasing both the electricity and the thermal energy prices, but the B-PTES configuration is mostly affected by the thermal energy price variation, while the RECB-PTES is visibly influenced also by the electricity price variation.

Results of this study can be a starting point for a deeper investigation on the integration of the system in a particular application with pre-determined electric and thermal demand profiles, and with a defined RES power plant.

REFERENCES

[1] A. Vecchi *et al.*, "Carnot Battery development: A review on system performance, applications and commercial state-of-the-art," *J. Energy Storage*, vol. 55, p. 105782, Nov. 2022, doi: 10.1016/j.est.2022.105782.

[2] Z. Song *et al.*, "Multi-objective optimization of a semi-active battery/supercapacitor energy storage system for electric vehicles," *Appl. Energy*, vol. 135, pp. 212–224, Dec. 2014, doi: 10.1016/j.apenergy.2014.06.087.

[3] F. Díaz-González, A. Sumper, O. Gomis-Bellmunt, and F. D. Bianchi, "Energy management of flywheel-based energy storage device for wind power smoothing," *Appl. Energy*, vol. 110, pp. 207–219, Oct. 2013, doi: 10.1016/j.apenergy.2013.04.029.

[4] C. S. Lai and M. D. McCulloch, "Levelized cost of electricity for solar photovoltaic and electrical energy storage," *Appl. Energy*, vol. 190, pp. 191–203, Mar. 2017, doi: 10.1016/j.apenergy.2016.12.153.

[5] O. Dumont, G. F. Frate, A. Pillai, S. Lecompte, M. De paepe, and V. Lemort, "Carnot battery technology: A state-of-the-art review," *J. Energy Storage*, vol. 32, p. 101756, Dec. 2020, doi: 10.1016/j.est.2020.101756.

[6] M. Gimeno-Gutiérrez and R. Lacal-Arántegui, "Assessment of the European potential for pumped hydropower energy storage based on two existing reservoirs," *Renew. Energy*, vol. 75, pp. 856–868, Mar. 2015, doi: 10.1016/j.renene.2014.10.068.

[7] Y. Luo, J. Andresen, H. Clarke, M. Rajendra, and M. Maroto-Valer, "A framework for waste heat energy recovery within data centre," *Energy Procedia*, vol. 158, pp. 3788–3794, Feb. 2019, doi: 10.1016/j.egypro.2019.01.875.

[8] A. Vecchi, Y. Li, Y. Ding, P. Mancarella, and A. Sciacovelli, "Liquid air energy storage (LAES): A review on technology state-of-the-art, integration pathways and future perspectives," *Adv. Appl. Energy*, vol. 3, p. 100047, Aug. 2021, doi: 10.1016/j.adapen.2021.100047.

[9] G. F. Frate, L. Ferrari, and U. Desideri, "Multi-criteria investigation of a pumped thermal electricity storage (PTES) system with thermal integration and sensible heat storage," *Energy Convers. Manag.*, vol. 208, p. 112530, Mar. 2020, doi: 10.1016/j.enconman.2020.112530.
[10] N. Torricelli, L. Branchini, A. De Pascale, O. Dumont, and V. Lemort, "Optimal Management of Reversible Heat Pump/Organic Rankine Cycle Carnot Batteries," *J. Eng. Gas Turbines Power*, vol. 145, no. 4, Dec. 2022, doi: 10.1115/1.4055708.
[11] M. Bianchi *et al.*, "Experimental analysis of a micro-ORC driven by piston expander for low-grade heat recovery," *Appl. Therm. Eng.*, vol. 148, pp. 1278–1291, Feb. 2019, doi: 10.1016/j.applthermaleng.2018.12.019.
[12] P. Vinnemeier, M. Wirsum, D. Malpiece, and R. Bove, "Integration of Pumped-Heat-Electricity-Storage into Water / Steam Cycles of Thermal Power Plants," p. 14.
[13] O. Dumont and V. Lemort, "Mapping of performance of pumped thermal energy storage (Carnot battery) using waste heat recovery," *Energy*, vol. 211, p. 118963, Nov. 2020, doi: 10.1016/j.energy.2020.118963.
[14] Y.-M. Kim, D.-G. Shin, S.-Y. Lee, and D. Favrat, "Isothermal transcritical CO2 cycles with TES (thermal energy storage) for electricity storage," *Energy*, vol. 49, pp. 484–501, Jan. 2013, doi: 10.1016/j.energy.2012.09.057.
[15] L. Sanz Garcia, E. Jacquemoud, and P. Jenny, *THERMO-ECONOMIC HEAT EXCHANGER OPTIMIZATION FOR ELECTRO-THERMAL ENERGY STORAGE BASED ON TRANSCRITICAL CO2 CYCLES*. 2019. doi: 10.17185/duepublico/48917.
[16] F. Ayachi, N. Tauveron, T. Tartière, D. Nguyen, H. Davarzani, and E. Macchi, "Inclusion of CO2 Transcritical Heat-Pump and Power Cycles in a Massive Electricity Storage System," Sep. 2016.
[17] M. Abarr, J. Hertzberg, and L. D. Montoya, "Pumped Thermal Energy Storage and Bottoming System Part B: Sensitivity analysis and baseline performance," *Energy*, vol. 119, pp. 601–611, Jan. 2017, doi: 10.1016/j.energy.2016.11.028.
[18] W. D. Steinmann, "The CHEST (Compressed Heat Energy STorage) concept for facility scale thermo mechanical energy storage," *Energy*, vol. 69, pp. 543–552, May 2014, doi: 10.1016/j.energy.2014.03.049.
[19] A. White, G. Parks, and C. N. Markides, "Thermodynamic analysis of pumped thermal electricity storage," *Appl. Therm. Eng.*, vol. 53, no. 2, pp. 291–298, May 2013, doi: 10.1016/j.applthermaleng.2012.03.030.
[20] L. Wang, X. Lin, L. Chai, L. Peng, D. Yu, and H. Chen, "Cyclic transient behavior of the Joule–Brayton based pumped heat electricity storage: Modeling and analysis," *Renew. Sustain. Energy Rev.*, vol. 111, pp. 523–534, Sep. 2019, doi: 10.1016/j.rser.2019.03.056.
[21] J. McTigue, P. Farres-Antunez, K. Ellingwood, T. Neises, and A. White, "Pumped thermal electricity storage with supercritical CO2 cycles and solar heat input," *AIP Conf. Proc.*, vol. 2303, no. 1, p. 190024, Dec. 2020, doi: 10.1063/5.0032337.
[22] A. Benato, "Performance and cost evaluation of an innovative Pumped Thermal Electricity Storage power system," *Energy*, vol. 138, pp. 419–436, Nov. 2017, doi: 10.1016/j.energy.2017.07.066.
[23] J. D. McTigue, A. J. White, and C. N. Markides, "Parametric studies and optimisation of pumped thermal electricity storage," *Appl. Energy*, vol. 137, pp. 800–811, Jan. 2015, doi: 10.1016/j.apenergy.2014.08.039.
[24] Thermoflex 30, 2022, Thermoflow Inc., Jeckconville FL.
[25] M. Krüger, "Brayton batteries for combined electricty and heat and cooling production: Systematic concept and parametric study," presented at the International Workshop on Carnot Batteries (IWCB), Stuttgart, Sep. 2022.

[26] S. Maccarini, S. Medhi, S. Barberis, L. Gini, and A. Traverso, "Thermoeconomic analysis of PTES layouts evolving sCO2 for industrial WHR integration," presented at the International Workshop on Carnot Batteries (IWCB), Stuttgart, Sep. 2022.
[27] V. Novotny, V. Basta, and J. Spale, "PTES with realistic components parameters - design, sizing & costing of a case scenario with Brayton packed bed and sCO2 systems," presented at the International Workshop on Carnot Batteries (IWCB), Stuttgart, Sep. 2022.
[28] S. Trevisan, R. Guedez, and B. Bjarke, "Techno-economic assessment of a Carnot battery for industrial application," presented at the International Workshop on Carnot Batteries (IWCB), Stuttgart, Sep. 2022.
[29] Eric W. Lemmon, Ian H. Bell, Marcia L. Huber, and Mark O. McLinden, "REFPROP 10.0 Standard Reference Database 23." National Institute of Standards and Technology, Boulder, Colorado, United States.
[30] A. M. Ancona *et al.*, "A Comparison Between Organic Rankine Cycle and Supercritical CO2 Bottoming Cycles for Energy Recovery From Industrial Gas Turbines Exhaust Gas," *J. Eng. Gas Turbines Power*, vol. 143, no. 12, Art. no. 12, Dec. 2021, doi: 10.1115/1.4051950.
[31] S. Lecompte, "Performance evaluation of organic Rankine cycle architectures : application to waste heat valorisation," dissertation, Ghent University, 2016. Accessed: Mar. 09, 2023. [Online]. Available: http://hdl.handle.net/1854/LU-7223134
[32] GSE, "Rapporto Statistico GSE - FER 2020," 2020. https://www.gse.it/documenti_site/Documenti%20GSE/Rapporti%20statistici/Rapporto%20Statistico%20GSE%20-%20FER%202020.pdf
[33] "GME - Gestore dei Mercati Energetici SpA." https://www.mercatoelettrico.org/It/Tools/Accessodati.aspx?ReturnUrl=%2fIt%2fdownload%2fDatiStorici.aspx (accessed Mar. 09, 2023).
[34] "Costi e tariffe del teleriscaldamento in Emilia Romagna." https://www.ilteleriscaldamento.eu/teleriscaldamento_emilia_romagna.htm (accessed Mar. 09, 2023).
[35] G. Angelino and C. Invernizzi, "Prospects for real-gas reversed Brayton cycle heat pumps," *Int. J. Refrig.*, vol. 18, no. 4, pp. 272–280, May 1995, doi: 10.1016/0140-7007(95)00005-V.
[36] *Directive 2004/8/EC of the European Parliament and of the Council of 11 February 2004 on the promotion of cogeneration based on a useful heat demand in the internal energy market and amending Directive 92/42/EEC*, vol. 052. 2004. Accessed: Dec. 14, 2022. [Online]. Available: http://data.europa.eu/eli/dir/2004/8/oj/eng
[37] C. Arpagaus, F. Bless, M. Uhlmann, J. Schiffmann, and S. S. Bertsch, "High temperature heat pumps: Market overview, state of the art, research status, refrigerants, and application potentials," *Energy*, vol. 152, pp. 985–1010, Jun. 2018, doi: 10.1016/j.energy.2018.03.166.
[38] G. F. Frate, M. Antonelli, and U. Desideri, "A novel Pumped Thermal Electricity Storage (PTES) system with thermal integration," *Appl. Therm. Eng.*, vol. 121, pp. 1051–1058, Jul. 2017, doi: 10.1016/j.applthermaleng.2017.04.127.